Published in final edited form as:
J Immunol. 2007 September 1; 179(5): 2731–2740.

Novel Exosome-Targeted CD4+ T Cell Vaccine Counteracting CD4+ 25+ Regulatory T Cell-Mediated Immune Suppression and Stimulating Efficient Central Memory CD8+ CTL Responses[1]

Siguo Hao[*], **Yongqing Liu**[*], **Jinying Yuan**[*], **Xueshu Zhang**[*], **Tianpei He**[*], **Xiaochu Wu**[†], **Yangdou Wei**[†], **Deming Sun**[‡], and **Jim Xiang**[*,2]

[*] *Department of Oncology and Immunology, University of Saskatchewan, Saskatoon, Saskatchewan, Canada*

[†] *Department of Biology, Research Unit, Division of Health Research, Saskatchewan Cancer Agency, University of Saskatchewan, Saskatoon, Saskatchewan, Canada*

[‡] *Kentucky Lions Eye Center, University of Louisville, Louisville, KY 40202*

Abstract

T cell-to-T cell Ag presentation is increasingly attracting attention. In this study, we demonstrated that active $CD4^+$ T (aT) cells with uptake of OVA-pulsed dendritic cell-derived exosome (EXO_{OVA}) express exosomal peptide/MHC class I and costimulatory molecules. These EXO_{OVA}-uptaken (targeted) $CD4^+$ aT cells can stimulate $CD8^+$ T cell proliferation and differentiation into central memory $CD8^+$ CTLs and induce more efficient in vivo antitumor immunity and long-term $CD8^+$ T cell memory responses than OVA-pulsed dendritic cells. They can also counteract $CD4^+25^+$ regulatory T cell-mediated suppression of in vitro $CD8^+$ T cell proliferation and in vivo $CD8^+$ CTL responses and antitumor immunity. We further elucidate that the EXO_{OVA}-uptaken (targeted)$CD4^+$ aT cell's stimulatory effect is mediated via its IL-2 secretion and acquired exosomal CD80 costimulation and is specifically delivered to $CD8^+$ T cells in vivo via acquired exosomal peptide/MHC class I complexes. Therefore, EXO-targeted active $CD4^+$ T cell vaccine may represent a novel and highly effective vaccine strategy for inducing immune responses against not only tumors, but also other infectious diseases.

Dendritic cells (DC)[3] process exogenous Ags in endosomal compartments such as multivesicular endosomes (1) which can fuse with plasma membrane, thereby releasing Ag-presenting vesicles called "exosomes" (EXO) (2,3). EXO are 50- to 90-nm diameter vesicles containing Ag-presenting (MHC class I, class II, CD1, heat shock protein 70–90), tetraspan (CD9, CD63, CD81), adhesion (CD11b, CD54), and costimulatory (CD86) molecules (4,5), i.e., the necessary machinery required for generating potent immune responses.

[1]This work was supported by Research Grants MOP 67230 and 79415 from the Canadian Institutes of Health Research. S.H. was supported by a Postdoctoral Fellowship from Saskatchewan Health Research Foundation.

2Address correspondence and reprint requests to Dr. Jim Xiang, Saskatoon Cancer Center, 20 Campus Drive, Saskatoon, Saskatchewan S7N 4H4, Canada. E-mail address: jxiang@scf.sk.ca.

Disclosures
The authors have no financial conflict of interest.

[3]Abbreviations used in this paper: DC, dendritic cell; EXO, exosome; pMHC, peptide/MHC; DC_{OVA}, OVA-pulsed DC; EXO_{OVA}, DC_{OVA}-derived EXO; aT, active $CD4^+$ T; aT_{EXO}, EXO_{OVA}-uptaken (targeted) aT; KO, knockout; EXO_{CFSE}, CFSE-labeled EXO; nT, naive OVA-specific T; Tr, regulatory T; nT_{EXO}, nT cocultured with EXO_{OVA}; Tm, memory T; emCTL, effector memory CTL; cmCTL, central memory CTL; ECD, energy-coupled dye.

Zitvogel et al. (3) first demonstrated vaccination of DC-derived EXO in eradication of tumors in animal models. Subsequently, EXO-based vaccines have been confirmed to stimulate strong CTL responses and induce antitumor immunity in different animal models (6,7). However, its therapeutic efficiency is still limited to only production of prophylactic immunity against tumors possibly due to lacking capacity of breaking immune tolerance (8). Exosomal peptide/MHC class I and II (pMHC I and II) complexes are functional, but require transfer to DC to promote T cell activation leading to tumor eradication (9–11). Therefore, the potential pathway of in vivo EXO-mediated antitumor immunity may be through uptake of EXO by host immature DC that, in turn, stimulate Ag-specific T lymphocytes via the pMHC complexes and costimulatory molecules on EXO-uptaken DC. In addition, Kennedy et al. (12) have also demonstrated that $CD4^+$ T cells can acquire APC membrane molecules in vivo and induce memory CTL responses. We have recently demonstrated that mature DC with uptake of OVA-pulsed DC (DC_{OVA})-derived EXO (EXO_{OVA}) express a higher level of pMHC I and costimulatory CD40, CD54, and CD80 molecules and can strongly stimulate OVA-specific $CD8^+$ CTL responses and antitumor immunity (13). Recently, we have also demonstrated that $CD4^+$ Th cells can acquire membrane molecules from DC via DC activation, and act as Th-APCs (14). These Th-APC with acquired pMHC I and costimulatory CD54 and CD80 molecules can stimulate tumor-specific $CD8^+$ CTL responses and induce antitumor immunity. One of the potential mechanisms of $CD4^+$ T cell acquisition of DC molecules is uptake of DC-released EXO by $CD4^+$ T cells. Therefore, these results clearly indicate that DC-derived EXO can transfer the Ag-presenting activity of DCs to either DC or $CD4^+$ T cells through EXO uptake by these cells. However, the EXO-targeted $CD4^+$ T cell vaccine and its potential immune mechanism in induction of antitumor CTL responses have not been studied and elucidated.

In this study, we demonstrated that EXO_{OVA}-uptaken (targeted) active $CD4^+$ T (aT_{EXO}) cells can 1) stimulate central memory $CD8^+$ CTL responses, more efficient antitumor immunity, and T cell memory than DC_{OVA} and 2) counteract $CD4^+25^+$ regulatory T (Tr) cell-mediated immune suppression. We also elucidated that the aT_{EXO} stimulatory effect is mediated via its IL-2 secretion and acquired exosomal CD80 costimulation and is specifically delivered to $CD8^+$ T cells in vivo via acquired exosomal pMHC I complexes.

Materials and Methods

Reagents, cell lines, and animals

OVA was obtained from Sigma-Aldrich. OVA I (SIINFEKL) and OVA II (ISQAVHAAHAEINEAGR) which are OVA peptides specific for H-$2K^b$ and Ia^b, respectively (15,16). Mut I (FEQNTAQP) peptide is specific for H-$2K^b$ of an irrelevant 3LL lung carcinoma (11). All peptides were synthesized by Multiple Peptide Systems. Biotin-labeled or FITC-labeled Abs specific for H-$2K^b$ (AF6-88.5), Ia^b (AF6-120.1), CD4 (GK1.5), CD8 (53-6.7), CD11c (HL3), CD25 (7D4), CD40 (IC10), CD44 (IM7), CD54 (3E2), CD62L (MEL-14), CD69 (H1.2F3), CD80 (16-10A1), IL-7R (4G3), and Vα2V$\beta5^+$ TCR (MR9-4), as well as FITC-conjugated avidin, were all obtained from BD Pharmingen. Anti-LFA-1 Ab, CTLA-4/Ig fusion protein, recombinant mouse IL-4, and GM-CSF were purchased from R&D Systems. The mouse thymoma cell line EL4 and OVA-transfected EL4 (EG7) cell line were obtained from American Type Culture Collection. The highly lung metastasis OVA-transfected BL6–10_{OVA} melanoma cell line was generated in our own laboratory (14). Female C57BL/6 (B6, $CD45.2^+$), C57BL/6.1 (B6.1, $CD45.1^+$), OVA-specific TCR-transgenic OT I and OT II mice, H-$2K^b$, Ia^b, IL-2, IFN-γ, TNF-α, CD40, CD54, and CD80 gene knockout (KO) mice were obtained from The Jackson Laboratory. Homozygous OT II/H-$2K^{b-/-}$, OT II/$CD40^{-/-}$, OT II/$CD54^{-/-}$, OT II/$CD80^{-/-}$, OT II/IL-$2^{-/-}$, OT II/IFN-γ, and OT II/TNF-α $^{-/-}$ mice were

generated by backcrossing the designated gene KO mice onto the OT II background. All mice were treated according to animal care committee guidelines of the University of Saskatchewan.

DC generation

DCs were generated as described previously (17). Briefly, spleen cells were prepared in PBS with 5 mM EDTA, washed, and incubated in culture medium with 7% FCS at 37°C for 2 h. Nonadherent cells were removed by gentle pipetting with warm serum-free medium. Adherent cells were cultured overnight in medium with 1% normal mouse serum, GM-CSF (1 ng/ml), and OVA (0.3 mg/ml). These DCs were termed as $DC_{OVA.}$ DC generated from H-2K^b, CD54, CD40, and CD80 gene KO mice were referred to as ($K^{b-/-}$)DC_{OVA}, ($CD40^{-/-}$)DC_{OVA}, ($CD54^{-/-}$)DC_{OVA} and ($CD80^{-/-}$)DC_{OVA}, respectively.

EXO preparation

Preparation and purification of EXO derived from the culture supernatants of DC_{OVA} were previously described (13), an overage of 5 μg of EXO was recovered from an overnight culture of 1×10^6 DC_{OVA} in 1.0 ml of AIM-V serum-free medium containing GM-CSF (10 ng/ml). EXO derived from DC_{OVA} were termed EXO_{OVA}. Similar to DC_{OVA}, EXO_{OVA} also expressed MHC class I (H-2K^b) and class II (Ia^b), CD11c, CD40, CD54, CD80, and the pMHC I complex, but in a lesser content, compared with DC_{OVA} (13). EXO derived from ($K^{b-/-}$) DC_{OVA}, ($CD40^{-/-}$)DC_{OVA}, ($CD54^{-/-}$) DC_{OVA}, and ($CD80^{-/-}$)DC_{OVA} were termed ($K_b^{-/-}$) $EXO_{OVA,}$ ($CD40^{-/-}$)EXO_{OVA}, ($CD54^{-/-}$)EXO_{OVA}, and ($CD80^{-/-}$)EXO_{OVA}, respectively. To generate CFSE-labeled EXO, DC_{OVA} were stained with 0.5 μM CFSE at 37°C for 20 min (16) and washed three times with PBS, and then pulsed with OVA protein in AIM-V serum-free medium overnight. The CFSE-labeled EXO (EXO_{CFSE}) was harvested and purified from the culture supernatants as previously described above.

CD4$^+$ T cell preparation and characterization

Naive OVA-specific T (nT) cells were isolated from OVA-specific TCR-transgenic OT I and OT II mouse spleens, enriched by passage through nylon wool columns (C&A Scientific), and then purified by negative selection using anti-mouse CD8(Ly2) or CD4 (L3T4) paramagnetic beads (Dynal Biotech) to yield populations that were >98% CD4$^+$/Vα2Vβ5$^+$ or CD8$^+$/Vα2Vβ5$^+$, respectively (14). To generate active OT II CD4$^+$ T cells, the spleen cells from OT II mice were cultured in RPMI 1640 medium containing IL-2 (20 U/ml) and Con A (1 μg/ml) for 3 days. The Con A-activated CD4$^+$ T (aT) cells were purified using nylon wool columns and then CD4 microbeads (Miltenyi Biotec). The CD4$^+$ aT cells derived from OT II/H-2K$^{b-/-}$, OT II/CD40$^{-/-}$, OT II/CD54$^{-/-}$, and OT II/ CD80$^{-/-}$mice were termed aT (H-2K$^{b-/-}$), aT(CD40$^{-/-}$), aT(CD54$^{-/-}$), and aT(CD80$^{-/-}$), respectively. The above naive and Con A-activated CD4$^+$ T cells were analyzed using a panel of Abs by flow cytometry. To assess the potential counteraction of CD4$^+$25$^+$ Tr cell-induced suppression by EXO-targeted CD4$^+$ T cells, CD4$^+$CD25$^+$ Tr cells were purified from C57BL/6 mouse spleen T cells using CD25 microbeads (clone 7D4; Milte-nyi Biotec) (18). The purified CD4$^+$CD25$^+$ Tr cells were stained with PE-anti-CD25 (clone PC61.5), FITC-CD4 (clone GK1.5), and energy-coupled dye (ECD)-Foxp3 (clone FJK-16S) using Regulatory T Cell Staining kit No. 3 (eBioscience), and then analyzed by flow cytometry.

Exosomal molecule uptake by CD4$^+$ T cells

First, the OT II CD4$^+$ nT and aT cells were incubated with EXO_{CFSE} (10 μg/1 $\times$ 10^6 T cells in 200 μl of AIM-V serum-free medium containing IL-2 (20 U/ml)) at 37°C for 5 h and then analyzed for CFSE staining by flow cytometry. In another set of experiments, the OT II CD4$^+$ aT cells were incubated with EXO_{CFSE} under the above same condition for 1, 3, and 5 h, and then assessed by confocal fluorescence microscopy. To further determine the transfer

of exosomal molecules to T cells, the $CD4^+$ nT and aT cells from OT II mice or OT II mice with different gene KO were incubated with EXO_{OVA}, and then analyzed for expression of H-$2K^b$, CD40, CD54, CD80, and pMHC I by flow cy-tometry or analyzed for expression of CD40 and CD80 by confocal fluorescence microscopy. The OT II $CD4^+$ nT and aT cells cocultured with EXO_{OVA} were termed nT_{EXO} and aT_{EXO} cells, respectively. The $CD4^+$ aT (H-$2K^{b-/-}$), aT($CD40^{-/-}$), aT($CD54^{-/-}$), and aT($CD80^{-/-}$) cells were cocultured with ($K^{b-/-}$) EXO_{OVA}, ($CD40^{-/-}$)EXO_{OVA}, ($CD54^{-/-}$)EXO_{OVA}, and ($CD80^{-/-}$)EXO_{OVA} and termed $CD4^+$ aT_{EXO} ($K^{b-/-}$), aT_{EXO}($CD40^{-/-}$), aT_{EXO}($CD54^{-/-}$), and aT_{EXO}($CD80^{-/-}$) cells, respectively. The $CD4^+$ aT cells from OT II/IL-$2^{-/-}$, OT II/ IFN-γ, and OT II/TNF-α $^{-/-}$ mice were cocultured with EXO_{OVA} and termed $CD4^+$ aT_{EXO}(IL-$2^{-/-}$), aT_{EXO}(IFN-γ $^{-/-}$), and aT_{EXO}(TNF-α $^{-/-}$) cells, respectively. The cytokine profiles of aT_{EXO}($K^{b-/-}$), aT_{EXO} ($CD40^{-/-}$), aT_{EXO}($CD54^{-/-}$), and aT_{EXO}($CD80^{-/-}$) cells are similar to that of aT_{EXO} cells, whereas the cytokine profiles of aT_{EXO}(IL-$2^{-/-}$), aT_{EXO}(IFN-γ $^{-/-}$), and aT_{EXO}(TNF-α $^{-/-}$) cells are also similar to that of aT_{EXO} cells except for the specific cytokine (IL-2 or IFN-γ or TNF-α) deficiency (data not shown). For blocking assays, OT II $CD4^+$ aT cells were incubated with anti-H-$2K^b$, anti-Ia^b, and anti-LFA-1 Abs (12 μg/ml) or CTLA-4/Ig (12 μg/ml), respectively, on ice for 30 min, then were cocultured with EXO_{CFSE} for 5 h at 37°C. The cells were harvested and analyzed for CFSE expression by flow cytometry.

T cell proliferation assays

To assess the functional effect of $CD4^+$ nT_{EXO} and aT_{EXO} cells, we performed an in vitro $CD8^+$ T cell proliferation assay. $CD4^+$ nT_{EXO} and aT_{EXO} (0.3×10^5 cells/well) cells derived from OT II mice and their 2-fold dilutions were cultured with a constant number of naive OT I $CD8^+$ T cells (1×10^5 cells/well) in presence or absence of $CD4^+CD25^+$ Tr cells (0.3×10^5 cells/well) derived from C57BL/6 mice. To examine the molecular mechanism, a panel of reagents including anti-H-$2K^b$, I-A^b, and LFA-1 Abs and CTLA-4/Ig fusion protein (each 10 μg/ml), a mixture of the above reagents (as mixed reagents), and a mixture of isotype-matched irrelevant Abs (as control reagents) were added to the cell cultures, respectively. After culturing for 3 days, thymidine incorporation was determined by liquid scintillation counting (19). In the in vivo OVA-specific $CD8^+$ T cell proliferation assay, C57BL/6 mice (six mice per group) were i.v. immunized with irradiated (4000 rad) stimulators including DC_{OVA}, $CD4^+$ aT_{EXO} cells (1×10^6 cells/mouse), or $CD4^+$ aT_{EXO} cells (1×10^6 cells/ mouse) with different gene KO. In another set of experiments, C57BL/6 mice (six mice per group) were i.v. immunized with irradiated (4000 rad) DC_{OVA}, $CD4^+$ aT, and aT_{EXO} cells (1×10^6 cells/mouse) alone or together with $CD4^+25^+$ Tr cells (3×10^6 cells/mouse). For evaluation of in vivo OVA-specific $CD8^+$ T cell proliferation, the tail blood samples derived from mice 6 days after immunization were incubated with PE-H-$2K^b$/ OVAI tetramer and FITC-anti-CD8 Ab (Beckman Coulter) and analyzed by flow cytometry (13).

Cytotoxicity assay

In vivo cytotoxicity assay was performed as previously described (14). Briefly, wild-type C57BL/6 or $Ia^{b-/-}$ mice (six mice per group) were i.v. immunized with the above stimulator cells (1×10^6 cells/mouse), respectively. In another set of experiments, C57BL/6 mice (six mice per group) were i.v. injected with irradiated (4000 rad) DC_{OVA} and $CD4^+$ aT_{EXO} cells (1×10^6 cells/mouse) alone or together with $CD4^+25^+$ Tr cells (3×10^6 cells/mouse). Splenocytes were harvested from naive mouse spleens and incubated with either high (3.0 μM, $CFSE^{high}$) or low (0.6 μM, $CFSE^{low}$) concentrations of CFSE, to generate differentially labeled target cells. The $CFSE^{high}$ cells were pulsed with OVA I peptide, whereas the $CFSE^{low}$ cells were pulsed with Mut 1 peptide and served as internal controls. These peptide-pulsed target cells were washed extensively to remove free peptides, and then i.v. coinjected at a 1:1 ratio into the immunized mice 6 days after immunization. Sixteen hours after the target

cell delivery, the spleens of immunized mice were removed and residual $CFSE^{high}$ and $CFSE^{low}$ target cells remaining in the recipients' spleens were analyzed by flow cytometry.

Animal studies

To examine the antitumor protective immunity conferred by EXO-targeted $CD4^+$ T cells, wild-type C57BL/6 mice ($n = 8$) were injected i.v. with irradiated (4000 rad) DC_{OVA}, aT, and aT_{EXO} cells (1×10^6 cells/mouse) with or without coinjection of $CD4^+25^+$ Tr cells (3×10^6 cells/mouse) aT_{EXO} cells with various gene KO (1×10^6 cells/mouse), respectively. The mice were injected with PBS as a control. To assess the antitumor immunity, the immunized mice were challenged i.v. with 0.5×10^6 $BL6–10_{OVA}$ tumor cells 6 days subsequent to the immunization. To assess the long-term antitumor immunity, wild-type C57BL/6 mice were first immunized with irradiated (4000 rad) DC_{OVA} and aT_{EXO} cells (1×10^6 cells/mouse). The immunized mice were then challenged i.v. with 2×10^6 $BL6–10_{OVA}$ cells 3 mo subsequent to the immunization to assess development of tumor-specific $CD8^+$ memory T (Tm) cells. The mice were sacrificed 4 wk after tumor cell injection and two individuals counted the lung metastasis tumor colonies in a blind fashion. $BL6–10_{OVA}$-derived metastases on freshly isolated lungs appeared as discrete black-pigmented foci that could be distinguishable from normal lung tissues and all were confirmed by histological examination. Metastasis foci too numerous to count were assigned an arbitrary value of >100 (14).

Results

$CD4^+$ T cells uptake exosomal pMHC I and costimulatory molecules in both Ag-specific and nonspecific manners

The nT and Con A-stimulated aT cells derived from transgenic OT II mice expressed both CD4 and TCR. The latter ones also expressed active T cell markers (CD25 and CD69) (Fig. 1) and secreted IL-2 (~2.4 ng/ml/10^6 cells/24 h), IFN-γ (~2.0 ng/ml/10^6 cells/24 h), and TNF-α (~1.7 ng/ml/10^6 cells/24 h), but no IL-4 and IL-10, indicating that they are active type Th1 cells. In addition, there was no CD11-positive splenic DC contamination in the purified $CD4^+$ aT population (Fig. 1). To assess EXO uptake, $CD4^+$ nT and aT cells derived from OT II and wild-type C57BL/6 (B6) mice were incubated with EXO_{CFSE} expressing CFSE (Fig. 2*a*) for various times and then analyzed by flow cytometry and confocal fluorescence microscopy. As shown in Fig. 2*a*, the CFSE dye was minimally and apparently detectable on OT II $CD4^+$ nT and aT cells, respectively. The uptake of EXO_{CFSE} by OT II $CD4^+$ aT cells increased with incubation time and reached a maximal level (80% CFSE-positive cells) after a 5-h incubation (Fig. 2*b*), which was also confirmed by confocal fluorescence microscopic analysis (Fig. 3*a*). The CFSE-positive cells declined with time when culturing them in medium, but were still detectable >3 days in culture, indicating that the uptaken exosomal molecules on $CD4^+$ T cells are quite stable, which is consistent with a previous report by Undale et al. (20). Similar to CFSE dye, other exosomal molecules such as $H\text{-}2K^b$, CD40, CD54, and CD80 molecules were also minimally and apparently transferred from EXO_{OVA} onto OT II $CD4^+$ nT and aT cells, respectively (Fig. 2, *c* and *e*). In addition, the pMHC I complexes were also transferred onto $CD4^+$ aT cells. To further confirm it, we incubated EXO_{OVA} with OT II $CD4^+$ T cells with different gene KO and then analyzed by flow cytometry or confocal fluorescence microscopy. The original OT II $CD4^+$ nT and aT cells with different gene KO did not express endogenous $H\text{-}2K^b$, CD40, CD54, and CD80, respectively. However, after incubation with EXO_{OVA}, T cells (especially the $CD4^+$ aT cells) did display the above exosomal molecules (Fig. 2, *d* and *f*), indicating that increased expression of the above molecules on $CD4^+$ T cells is due to an uptake of EXO molecules rather than an endogenous up-regulation. This was also confirmed by confocal fluorescence microscopic analysis. As shown in Fig. 3*b*, $CD4^+$ aT cells with deficiency of endogenous CD40 and CD80 expression displayed CD40 and CD80 expression after uptake of EXO_{OVA}. To elucidate the molecular mechanism involved in EXO uptake, we

used a panel of reagents in a blocking assay. The anti-Ia^b and LFA-1 Abs, but not the CTLA-4/Ig fusion protein and the anti-H-$2K^b$ Ab, were able to significantly block EXO uptake ($p < 0.05$) (Fig. 2*g*). This was further confirmed by a significant decrease in EXO uptake ($p < 0.05$) when incubation of aT($CD54^{-/-}$), but not aT($CD40^{-/-}$) and aT($CD80^{-/-}$), cells with EXO_{CFSE} derived from CFSE-labeled ($CD54^{-/-}$)DC_{OVA}, ($CD40^{-/-}$)DC_{OVA}, and ($CD80^{-/-}$)DC_{OVA}, respectively, indicating that the EXO_{OVA} uptake by $CD4^+$ T cells is mediated by both OVA-specific Ia^b/TCR and nonspecific CD54/LFA-1 interactions, but not by H-$2K^b$/TCR and CD80/CD28 interactions, which is consistent with previous reports by Hwang et al. (21,22).

$CD4^+$ aT_{EXO} cells counteract in vitro $CD4^+25^+$ Tr cell-mediated suppression of naive $CD8^+$ T cell proliferation

We then examined the stimulatory effect of EXO_{OVA}-targeted active $CD4^+$ T (aT_{EXO}) cells. As shown in Fig. 4*a*, EXO_{OVA} could prime $CD8^+$ T cell proliferation in vitro, which is consistent with previous reports by Hwang et al. (21,22), but in to a lesser extent compared with DC_{OVA}. Of interest, $CD4^+$ aT_{EXO} is a stronger stimulator in $CD8^+$ T cell proliferation than DC_{OVA}, whereas nT_{EXO} is a relatively weak stimulator. $CD4^+25^+$ Tr cells expressing CD4, CD25, and Foxp3 (Fig. 4*b*) inhibited DC_{OVA}-stimulated $CD8^+$ T cell proliferation (Fig. 4*a*). However, aT_{EXO} cells maintained their stimulatory effect in presence of $CD4^+25^+$ Tr cells, indicating that aT_{EXO} cells can counteract in vitro $CD4^+25^+$ Tr cell-mediated suppression of naive $CD8^+$ T cell proliferation.

$CD4^+$ aT_{EXO} cells stimulate in vitro $CD8^+$ T cell proliferation and differentiation into central memory T cells

We next conducted phenotypic characterization of the above in vitro aT_{EXO}-primed $CD8^+$ T cells. Our data showed that DC_{OVA} or aT_{EXO} priming resulted in several cycles of $CD8^+$ CFSE-T cell division, whereas nontreated $CD8^+$ CFSE-T cells were not divided (Fig. 4*c*). The primed T cells displayed expression of CD25, CD44 (Tm marker) (23) and CD62L (Fig. 4*c*). However, aT_{EXO}-primed $CD8^+$ T cells expressed IL-7R and higher CD62L than DC_{OVA}-primed ones with no IL-7R expression, indicating that they may be prone to becoming long-lived Tm cells. We then examined whether aT_{EXO}-primed CTL exhibited any other functional traits attributed to typical Tm cells. These traits include 1) secretion of IFN-γ upon Ag stimulation, 2) the enhanced survival and proliferation in response to IL-7 (24), and 3) the capacity to generate Ag-specific CTL. Our data showed that both DC_{OVA}- and aT_{EXO}-primed $CD8^+$ T cells secrete IFN-γ upon Ag stimulation by EG7 tumor cells expressing OVA (Fig. 4*d*). However, aT_{EXO}-primed CTL expanded better in the presence of IL-2 and IL-7 than DC_{OVA}-primed ones (Fig. 4*e*). In a chromium release assay, aT_{EXO}-primed CTL (aT_{EXO}/OT $I_{6.1}$) showed cytotoxicity to EG7 tumor cells, but at a relatively lower level than DC_{OVA}-primed ones (DC_{OVA}/OT $I_{6.1}$) (Fig. 4*f*). In addition, the nontreated OT $I_{6.1}$ cells used as a control did not show any killing activity to EG7 tumor cells. Taken together, our results indicate that DC_{OVA}-primed $CD44^+CD62L^{low}$IL-$7R^-$and aT_{EXO}-primed $CD44^+CD62L^{high}$IL-$7R^+$ CTL, which have high and low cytotoxicity to tumor cells, are consistent with typical effector and central memory CTL (emCTL and cmCTL), respectively (12,25).

$CD4^+$ aT_{EXO} cells stimulate in vivo $CD4^+$ T cell-independent $CD8^+$ T cell proliferation

We then performed a tetramer staining assay to detect OVA-specific $CD8^+$ T cells in wild-type C57BL/6 (B6) or MHC class II (Ia^b) gene KO mice. As shown in Fig. 5*a*, DC_{OVA} and aT_{EXO} cells stimulated proliferation of H-$2K^b$ /$OVA_{257–264}$ tetramer-positive $CD8^+$ T cells accounting for 1.03 and 2.24% of the total spleen $CD8^+$ T cell population in B6 mice, respectively, indicating that aT_{EXO} is a significantly stronger stimulator than DC_{OVA} ($p < 0.05$). In Ia^b gene KO mice lacking $CD4^+$ T cells, however, only aT_{EXO} cells (2.01%), but not DC_{OVA}, could stimulate OVA-specific $CD8^+$ T cell responses, indicating that the aT_{EXO}-

induced $CD8^+$ T cell response is $CD4^+$ T cell independent, whereas those of DC_{OVA} are $CD4^+$ T cell dependent.

$CD4^+$ aT_{EXO} cell-induced CTL responses and antitumor immunity are mediated by IL-2 and acquired exosomal CD80 specifically delivered via acquired exosomal pMHC I

To elucidate the immune mechanism involved in aT_{EXO}-induced CTL responses, we performed animal studies by using aT_{EXO} with different gene KO. The stimulation of OVA-specific $CD8^+$ T cell responses by $aT_{EXO}(CD54^{-/-})$ was reduced to more than half (1.08%) of the original one by aT_{EXO} (2.24%) (Fig. 5*b*), possibly due to lacking CD54/LFA-1 interaction leading to decreased EXO uptake by $aT_{EXO}(CD54^{-/-})$ cells. Interestingly, the stimulation of OVA-specific $CD8^+$ T cell responses by $aT_{EXO}(IL\text{-}2^{-/-})$ (0.24%) and $aT_{EXO}(CD80^{-/-})$ (0.42%) cells, but not by $aT_{EXO}(IFN\text{-}\gamma^{-/-})$ (2.15%), $aT_{EXO}(TNF\text{-}\alpha^{-/-})$ (2.13%) and $aT_{EXO}(CD40^{-/-})$ (2.21%), was greatly lost and significantly less than that by aT_{EXO} ($p < 0.05$), indicating that the aT_{EXO} stimulatory effect is mediated by its IL-2 and acquired CD80. Furthermore, $aT_{EXO}(K^{b-/-})$ cells (0.11%) with similar cytokine profiles as aT_{EXO}, but without acquired pMHC I complexes, also completely lost their stimulatory effect, indicating that the aT_{EXO} stimulatory effect is specifically delivered to $CD8^+$ T cells in vivo via acquired exosomal pMHC I complexes. To assess aT_{EXO}-induced $CD8^+$ T cell differentiation into CTL, we adoptively transferred OVAI peptide-pulsed splenocytes that had been strongly labeled with CFSE ($CFSE^{high}$), as well as the control peptide Mut 1-pulsed splenocytes that had been weakly labeled with CFSE ($CFSE^{low}$), into the recipient mice that had been vaccinated with DC_{OVA} and $CD4^+$ aT_{EXO} cells, respectively. As expected, the mice immunized with aT_{EXO} had larger loss of $CFSE^{high}$ cells than DC_{OVA} (75%) and $CD4^+$ aT_{EXO} cells (88%) (Fig. 5*c*), indicating that $CD4^+$ aT_{EXO} cells can most efficiently stimulate $CD8^+$ T cell differentiation into CTL effectors. Interestingly, the OVA-specific cytotoxicity was substantially lost in $CD4^+$ $aT_{EXO}(IL\text{-}2^{-/-})$-(2%) and aT_{EXO} $(CD80^{-/-})$-immunized (15%) mice and significantly less than the $CD4^+$ aT_{EXO}-induced one ($p < 0.05$), but not in $CD4^+$ aT_{EXO} $(IFN\text{-}\gamma^{-/-})$-(89%), $aT_{EXO}(TNF\text{-}\alpha^{-/-})$-(90%), and aT_{EXO} $(CD40^{-/-})$-immunized (88%) mice, thus further confirming that $CD4^+$ the aT_{EXO} stimulatory effect is mediated by its IL-2 secretion and acquired CD80 costimulation. In addition, the $CD4^+$ $aT_{EXO}(K^{b-/-})$-vaccinated mice did not display any killing activity (3%), again confirming that the acquired pMHC I complexes play a critical role in targeting the $CD4^+$ aT_{EXO} stimulatory effect to OVA-specific $CD8^+$ T cells in vivo. Furthermore, the results derived from our in vivo antitumor immunity studies are also consistent with the above aT_{EXO}-induced in vivo $CD8^+$ CTL responses (Fig. 5*a*). Our data showed that 1) $CD4^+$ aT_{EXO} cells induced stronger antitumor immunity than DC_{OVA} (Expt. I of Table I), and 2) IL-2 and acquired exosomal CD80 of $CD4^+$ aT_{EXO} are specifically delivered to $CD8^+$ T cells in vivo via acquired exosomal pMHC I (Expt. II of Table I).

$CD4^+$ aT_{EXO} cells induce efficient long-term OVA-specific $CD8^+$ T cell memory

Active $CD8^+$ T cells can become long-lived Tm cells after adoptive transfer in vivo (26). We then assessed whether these $CD4^+$ aT_{EXO}-primed $CD8^+$T cells can also become long-lived Tm cells. As shown in Fig. 6*a*, we still detected 0.46% OVA-specific $CD8^+$ T cells in peripheral blood of mice immunized with aT_{EXO}, which is significantly stronger than that (0.12%) in mice immunized with DC_{OVA} 3 mo after the immunization ($p < 0.05$). These OVA-specific $CD8^+$ T cells were also $CD44^+$, indicating that they are OVA-specific $CD8^+$ Tm cells. In addition, the survived $CD4^+$ aT_{EXO}-primed $CD8^+$ Tm cells are nearly 4-fold compared with the survived DC_{OVA}-stimulated ones, indicating that $CD4^+$ aT_{EXO}-primed $CD44^+CD62L^{high}IL\text{-}7R^+$ CTL with low cytotoxicity to tumor cells are long survival cmCTL. The recall responses were then assessed on day 4 after the boost of immunized mice with DC_{OVA}. As expected, $CD8^+$ Tm cells were expanded by 10-fold in these immunized mice after the boost (Fig. 6*b*), indicating that these $CD8^+$ Tm cells are functional. In another set of experiments, the above immunized mice were challenged with a high dose (2×10^6 cells/

mouse) of BL6–10_{OVA} tumor cells. Only four of eight (50%) mice immunized with DC_{OVA} were tumor free, whereas all eight of eight (100%) mice immunized with $CD4^+$ aT_{EXO} cells did not have any lung metastasis (Expt. III of Table I), indicating that $CD4^+$ aT_{EXO} cells can induce more efficient long-term $CD8^+$ T cell memory than DC_{OVA}.

$CD4^+$ aT_{EXO} cells counteract in vivo $CD4^+25^+$ Tr cell-mediated suppression of OVA-specific $CD8^+$ T cell proliferation and antitumor immunity

Because we demonstrated above the counteraction of in vitro $CD4^+25^+$ Tr cell-mediated suppression, we wanted to further assess the potential effect of $CD4^+$ aT_{EXO} cells in counteraction of in vivo $CD4^+25^+$ Tr cell-mediated suppression. We performed in vivo proliferation and cytotoxicity assays as described above. As shown in Fig. 7*a*, the stimulation of OVA-specific $CD8^+$ T cell responses in mice by DC_{OVA} (1.03%) was almost completely lost (0.10%) when mice were coinjected with $CD4^+25^+$ Tr cells ($p < 0.05$), indicating that $CD4^+25^+$ Tr cells can significantly inhibit DC_{OVA}-stimulated $CD8^+$T cell responses. However, the OVA-specific $CD8^+$ T cell responses in mice with $CD4^+$ aT_{EXO} stimulation in presence or absence of $CD4^+25^+$ Tr cells maintained at a similar level (2.24%). In the in vivo cytotoxicity assay, the effector CTL responses derived from DC_{OVA}, but not $CD4^+$ aT_{EXO} cells, in presence of $CD4^+25^+$ Tr cells were lost (Fig. 7*b*). Furthermore, the results derived from our in vivo antitumor immunity studies (Expt. IV of Table I) are also consistent with the above aT_{EXO}-induced in vivo $CD8^+$ CTL responses (Fig. 5). Our data demonstrated that $CD4^+$ aT_{EXO} cells, but not DC_{OVA}, induced efficient antitumor immunity in mice even with coinjection of $CD4^+25^+$ Tr cells, which was against the challenge of BL6–10_{OVA} tumor cells from developing lung tumor metastasis (Expt. IV of Table I), indicating that $CD4^+$ aT_{EXO} cells can counteract in vivo $CD4^+25^+$ Tr cell-mediated immune suppression, possibly through bypassing the $CD4^+25^+$ Tr cell-mediated suppressive pathway.

Discussion

According to the progressive linear differentiation hypothesis (27), T cell differentiation involves a phase of proliferation preceding the acquisition of fitness and effector function. Primed $CD8^+$ T cells reach a variety of differentiation stages that contain effector cells as well as cells that have been arrested at intermediate levels of differentiation. Thus, they retain a flexible gene imprinting. T cells that may survive after the retraction phase of an immune response can be resolved into distinct subsets of either cmCTLs representing cells at intermediate levels of differentiation or fully differentiated emCTLs with effector capacity (28,29). It has been shown that a strong Ag presentation stimulates development of effector CTL, whereas a less efficient Ag presentation can lead to generation of central memory CTL (30). In this study, we demonstrated that $CD4^+$ aT_{EXO} cells were able to stimulate naive $CD8^+$ T cell differentiation into $CD8^+44^+62^{high}$IL-$7R^+$ cmCTLs with less cytotoxicity and longer survival capacity leading to strong memory T cell responses, compared with DC_{OVA}-primed $CD8^+44^+62^{low}$IL-$7R^+$ emCTLs with high cytotoxicity and shorter survival capacity in vivo. Therefore, an EXO-targeted $CD4^+$ T cell vaccine using peripheral blood $CD4^+$ T cells of a cancer patient incubated with tumor cell-derived EXO from ascites of a cancer patient may be a useful strategy for EXO-based treatment of cancer.

Administration of attenuated T lymphocytes to animals has been shown to stimulate immune suppression and to prevent the development of experimental autoimmune diseases (31,32). Vaccination using myelin basic protein autoreactive T cells has also been applied to clinical trial in multiple sclerosis (33). In this study, we clearly showed that $CD4^+$ aT_{EXO} cells can more strongly stimulate OVA-specific immunogenic $CD8^+$ CTL responses, antitumor immunity, and $CD8^+$ T cell memory in wild-type mice than EXO and DC_{OVA}. Interestingly, the $CD8^+$CTL responses stimulated by are found to be $CD4^+$T cell independent. Thus, EXO-

aT_{EXO} targeted T cell vaccines may be very useful in induction of anti-HIV immunity in HIV patients with $CD4^+$ T cell deficiency because HIV-1 infection is characterized by a gradual loss of $CD4^+$ T cells and progressive immune deficiency (34). Furthermore, we also elucidated the molecular mechanism involved in aT_{EXO} vaccines, which includes 1) the IL-2 secretion and the acquired exosomal CD80 costimulation that mediate the aT_{EXO} stimulatory effect and 2) the acquired exosomal pMHC I complexes that play a critical role in targeting the aT_{EXO} stimulatory effect to $CD8^+$ T cells in vivo.

$CD4^+25^+$ Tr cells develop in the thymus and then enter peripheral tissues where they suppress activation of other self-reactive T cells (35,36). It has been reported that an elevated number of Tr cells was detected in tumors (37,38) which suppressed the anti-tumor immune responses by inhibition of $CD4^+$T cell proliferation and a helper effect (39–41) as well as DC maturation (42). Therefore, how to combat immune tolerance becomes a critical challenge in cancer immunotherapy (43). A variety of stimuli that increase the potency of T cell stimulation have been shown to abrogate $CD4^+$ Tr cell function including high Ag dose, TLR signals, CD28 engagement, and provision of IL-2 (44–48). In this study, we demonstrated that $CD4^+$ aT_{EXO} cells, but not DC_{OVA}, can stimulate $CD8^+$ T cell proliferation in the presence of $CD4^+25^+$ Tr cells in vitro and in vivo. These $CD4^+$ aT_{EXO} cells expressing exosomal pMHC I and CD80 and secreting IL-2 can break Tr cell-mediated immune tolerance, possibly due to its capacity to 1) directly stimulate $CD8^+$ T cell responses in absence of $CD4^+$ Th cells and DC, thus bypassing the above Tr cell-mediated suppressive pathways or 2) directly counteract $CD4^+$ Tr suppression via CD28 engagement and IL-2 stimulation (44–48).

Taken together, our data show that DC_{OVA}-derived EXO_{OVA} can be uptaken by $CD4^+$ T cells. EXO_{OVA}-targeted $CD4^+$ aT_{EXO} cells expressing acquired exosomal pMHC I and CD80 can stimulate $CD8^+$ cmCTL responses, more efficient in vivo antitumor immunity and long-term $CD8^+$ T cell memory than DC_{OVA}, and counteract $CD4^+25^+$ Tr cell-mediated suppression of OVA-specific CTL responses and antitumor immunity. The aT_{EXO} stimulatory effect is mediated via its IL-2 secretion and acquired exosomal CD80 costimulation and is specifically targeted to $CD8^+$T cells in vivo via acquired exosomal pMHC I complexes. Therefore, an EXO-targeted active $CD4^+$ T cell vaccine may represent a novel and highly effective vaccine strategy for inducing immune responses not only against tumors, but also other infectious diseases.

Acknowledgements

We appreciate Mark Boyd for help in flow cytometry.

References

1. Guermonprez P, Saveanu L, Kleijmeer M, Davoust J, Van Endert P, Amigorena S. ER-phagosome fusion defines an MHC class I cross-presentation compartment in dendritic cells. Nature 2003;425:397–402. [PubMed: 14508489]
2. Kleijmeer MJ, Escola JM, UytdeHaag FG, Jakobson E, Griffith JM, Osterhaus AD, Stoorvogel W, Melief CJ, Rabouille C, Geuze HJ. Antigen loading of MHC class I molecules in the endocytic tract. Traffic 2001;2:124–137. [PubMed: 11247303]
3. Zitvogel L, Regnault A, Lozier A, Wolfers J, Flament C, Tenza D, Ricciardi-Castagnoli P, Raposo G, Amigorena S. Eradication of established murine tumors using a novel cell-free vaccine: dendritic cell-derived exosomes. Nat Med 1998;4:594–600. [PubMed: 9585234]
4. Denzer K, Kleijmeer MJ, Heijnen HF, Stoorvogel W, Geuze HJ. Exosome: from internal vesicle of the multivesicular body to intercellular signaling device. J Cell Sci 2000;113(Pt 19):3365–3374. [PubMed: 10984428]
5. Clayton A, Court J, Navabi H, Adams M, Mason MD, Hobot JA, Newman GR, Jasani B. Analysis of antigen presenting cell derived exosomes, based on immuno-magnetic isolation and flow cytometry. J Immunol Methods 2001;247:163–174. [PubMed: 11150547]

6. Chaput N, Schartz NE, Andre F, Taieb J, Novault S, Bonnaventure P, Aubert N, Bernard J, Lemonnier F, Merad M, et al. Exosomes as potent cell-free peptide-based vaccine. II. Exosomes in CpG adjuvants efficiently prime naive Tc1 lymphocytes leading to tumor rejection. J Immunol 2004;172:2137–2146. [PubMed: 14764679]
7. Cho JA, Yeo DJ, Son HY, Kim HW, Jung DS, Ko JK, Koh JS, Kim YN, Kim CW. Exosomes: a new delivery system for tumor antigens in cancer immunotherapy. Int J Cancer 2005;114:613–622. [PubMed: 15609328]
8. Banchereau J, Steinman RM. Dendritic cells and the control of immunity. Nature 1998;392:245–252. [PubMed: 9521319]
9. Andre F, Chaput N, Schartz NE, Flament C, Aubert N, Bernard J, Lemonnier F, Raposo G, Escudier B, Hsu DH, et al. Exosomes as potent cell-free peptide-based vaccine. I. Dendritic cell-derived exosomes transfer functional MHC class I/peptide complexes to dendritic cells. J Immunol 2004;172:2126–2136. [PubMed: 14764678]
10. Thery C, Duban L, Segura E, Veron P, Lantz O, Amigorena S. Indirect activation of naive $CD4^+$ T cells by dendritic cell-derived exosomes. Nat Immunol 2002;3:1156–1162. [PubMed: 12426563]
11. Vincent-Schneider H, Stumptner-Cuvelette P, Lankar D, Pain S, Raposo G, Benaroch P, Bonnerot C. Exosomes bearing HLA-DR1 molecules need dendritic cells to efficiently stimulate specific T cells. Int Immunol 2002;14:713–722. [PubMed: 12096030]
12. Kennedy R, Undale AH, Kieper WC, Block MS, Pease LR, Celis E. Direct cross-priming by Th lymphocytes generates memory cytotoxic T cell responses. J Immunol 2005;174:3967–3977. [PubMed: 15778353]
13. Hao S, Bai O, Li F, Yuan J, Laferte S, Xiang J. Mature dendritic cells pulsed with exosomes stimulate efficient cytotoxic T-lymphocyte responses and antitumour immunity. Immunology 2007;120:90–102. [PubMed: 17073943]
14. Xiang J, Huang H, Liu Y. A new dynamic model of $CD8^+$ T effector cell responses via $CD4^+$ T helper-antigen-presenting cells. J Immunol 2005;174:7497–7505. [PubMed: 15944248]
15. Slingluff CL Jr. Tumor antigens and tumor vaccines: peptides as immunogens. Semin Surg Oncol 1996;12:446–453. [PubMed: 8914209]
16. Li M, Davey GM, Sutherland RM, Kurts C, Lew AM, Hirst C, Carbone FR, Heath WR. Cell-associated ovalbumin is cross-presented much more efficiently than soluble ovalbumin in vivo. J Immunol 2001;166:6099–6103. [PubMed: 11342628]
17. Zhang X, Huang H, Yuan J, Sun D, Hou WS, Gordon J, Xiang J. $CD4^-8^-$ dendritic cells prime $CD4^+$ T regulatory 1 cells to suppress antitumor immunity. J Immunol 2005;175:2931–2937. [PubMed: 16116179]
18. Shimizu J, Moriizumi E. $CD4^+CD25^-$ T cells in aged mice are hyporesponsive and exhibit suppressive activity. J Immunol 2003;170:1675–1682. [PubMed: 12574330]
19. Zhang W, Chen Z, Li F, Kamencic H, Juurlink B, Gordon JR, Xiang J. Tumour necrosis factor-α (TNF-α) transgene-expressing dendritic cells (DCs) undergo augmented cellular maturation and induce more robust T-cell activation and anti-tumour immunity than DCs generated in recombinant TNF-α. Immunology 2003;108:177–188. [PubMed: 12562326]
20. Undale AH, van den Elsen PJ, Celis E. Antigen-independent acquisition of MHC class II molecules by human T lymphocytes. Int Immunol 2004;16:1523–1533. [PubMed: 15351785]
21. Hwang I, Huang JF, Kishimoto H, Brunmark A, Peterson PA, Jackson MR, Surh CD, Cai Z, Sprent J. T cells can use either T cell receptor or CD28 receptors to absorb and internalize cell surface molecules derived from antigen-presenting cells. J Exp Med 2000;191:1137–1148. [PubMed: 10748232]
22. Hwang I, Sprent J. Role of the actin cytoskeleton in T cell absorption and internalization of ligands from APC. J Immunol 2001;166:5099–5107. [PubMed: 11290791]
23. Dutton RW, Bradley LM, Swain SL. T cell memory. Annu Rev Immunol 1998;16:201–223. [PubMed: 9597129]
24. Tan JT, Ernst B, Kieper WC, LeRoy E, Sprent J, Surh CD. Interleukin (IL)-15 and IL-7 jointly regulate homeostatic proliferation of memory phenotype $CD8^+$ cells but are not required for memory phenotype $CD4^+$ cells. J Exp Med 2002;195:1523–1532. [PubMed: 12070280]

25. Kaech SM, Tan JT, Wherry EJ, Konieczny BT, Surh CD, Ahmed R. Selective expression of the interleukin 7 receptor identifies effector CD8 T cells that give rise to long-lived memory cells. Nat Immunol 2003;4:1191–1198. [PubMed: 14625547]
26. Shi M, Xiang J. $CD4^+$ T cell-independent maintenance and expansion of memory $CD8^+$ T cells derived from in vitro dendritic cell activation. Int Immunol 2006;18:887–895. [PubMed: 16621867]
27. Lanzavecchia A, Sallusto F. Progressive differentiation and selection of the fittest in the immune response. Nat Rev Immunol 2002;2:982–987. [PubMed: 12461571]
28. Geginat J, Lanzavecchia A, Sallusto F. Proliferation and differentiation potential of human $CD8^+$ memory T-cell subsets in response to antigen or homeostatic cytokines. Blood 2003;101:4260–4266. [PubMed: 12576317]
29. Schwendemann J, Choi C, Schirrmacher V, Beckhove P. Dynamic differentiation of activated human peripheral blood $CD8^+$ and $CD4^+$ effector memory T cells. J Immunol 2005;175:1433–1439. [PubMed: 16034079]
30. van Faassen H, Saldanha M, Gilbertson D, Dudani R, Krishnan L, Sad S. Reducing the stimulation of $CD8^+$ T cells during infection with intracellular bacteria promotes differentiation primarily into a central ($CD62L^{high}$ $CD44^{high}$) subset. J Immunol 2005;174:5341–5350. [PubMed: 15843531]
31. Shapira OM, Mor E, Reshef T, Pfeffermann RA, Cohen IR. Prolongation of survival of rat cardiac allografts by T cell vaccination. J Clin Invest 1993;91:388–390. [PubMed: 8432846]
32. Kishimoto C, Takada H, Hiraoka Y, Shinohara H, Kitazawa M. Protection against murine coxsackievirus B3 myocarditis by T cell vaccination. J Mol Cell Cardiol 2000;32:2269–2277. [PubMed: 11113002]
33. Hong J, Zang YC, Nie H, Zhang JZ. $CD4^+$ regulatory T cell responses induced by T cell vaccination in patients with multiple sclerosis. Proc Natl Acad Sci USA 2006;103:5024–5029. [PubMed: 16547138]
34. Hazenberg MD, Hamann D, Schuitemaker H, Miedema F. T cell depletion in HIV-1 infection: how $CD4^+$ T cells go out of stock. Nat Immunol 2000;1:285–289. [PubMed: 11017098]
35. Bluestone JA, Abbas AK. Natural versus adaptive regulatory T cells. Nat Rev Immunol 2003;3:253–257. [PubMed: 12658273]
36. Cozzo C, Larkin J 3rd, Caton AJ. Cutting edge: self-peptides drive the peripheral expansion of $CD4^+CD25^+$ regulatory T cells. J Immunol 2003;171:5678–5682. [PubMed: 14634074]
37. Liyanage UK, Moore TT, Joo HG, Tanaka Y, Herrmann V, Doherty G, Drebin JA, Strasberg SM, Eberlein TJ, Goedegebuure PS, Linehan DC. Prevalence of regulatory T cells is increased in peripheral blood and tumor microenvironment of patients with pancreas or breast adeno-carcinoma. J Immunol 2002;169:2756–2761. [PubMed: 12193750]
38. Curiel TJ, Coukos G, Zou L, Alvarez X, Cheng P, Mottram P, Evdemon-Hogan M, Conejo-Garcia JR, Zhang L, Burow M, et al. Specific recruitment of regulatory T cells in ovarian carcinoma fosters immune privilege and predicts reduced survival. Nat Med 2004;10:942–949. [PubMed: 15322536]
39. Levings MK, Sangregorio R, Roncarolo MG. Human $CD25^+CD4^+$ T regulatory cells suppress naive and memory T cell proliferation and can be expanded in vitro without loss of function. J Exp Med 2001;193:1295–1302. [PubMed: 11390436]
40. Martin B, Banz A, Bienvenu B, Cordier C, Dautigny N, Becourt C, Lucas B. Suppression of $CD4^+$ T lymphocyte effector functions by $CD4^+CD25^+$ cells in vivo. J Immunol 2004;172:3391–3398. [PubMed: 15004137]
41. Nishikawa H, Jager E, Ritter G, Old LJ, Gnjatic S. $CD4^+CD25^+$ regulatory T cells control the induction of antigen-specific $CD4^+$ helper T cell responses in cancer patients. Blood 2005;106:1008–1011. [PubMed: 15840697]
42. Misra N, Bayry J, Lacroix-Desmazes S, Kazatchkine MD, Kaveri SV. Cutting edge: human $CD4^+CD25^+$ T cells restrain the maturation and antigen-presenting function of dendritic cells. J Immunol 2004;172:4676–4680. [PubMed: 15067041]
43. Pardoll DM. Cancer vaccines. Nat Med 1998;4:525–531. [PubMed: 9585204]
44. Thornton AM, Shevach EM. $CD4^+CD25^+$ immunoregulatory T cells suppress polyclonal T cell activation in vitro by inhibiting interleukin 2 production. J Exp Med 1998;188:287–296. [PubMed: 9670041]

45. Takahashi T, Kuniyasu Y, Toda M, Sakaguchi N, Itoh M, Iwata M, Shimizu J, Sakaguchi S. Immunologic self-tolerance maintained by $CD25^{+}CD4^{+}$ naturally anergic and suppressive T cells: induction of autoimmune disease by breaking their anergic/suppressive state. Int Immunol 1998;10:1969–1980. [PubMed: 9885918]

46. George TC, Bilsborough J, Viney JL, Norment AM. High antigen dose and activated dendritic cells enable Th cells to escape regulatory T cell-mediated suppression in vitro. Eur J Immunol 2003;33:502–511. [PubMed: 12645949]

47. Pasare C, Medzhitov R. Toll pathway-dependent blockade of $CD4^{+}CD25^{+}$ T cell-mediated suppression by dendritic cells. Science 2003;299:1033–1036. [PubMed: 12532024]

48. Sojka DK, Hughson A, Sukiennicki TL, Fowell DJ. Early kinetic window of target T cell susceptibility to $CD25^{+}$ regulatory T cell activity. J Immunol 2005;175:7274–7280. [PubMed: 16301632]

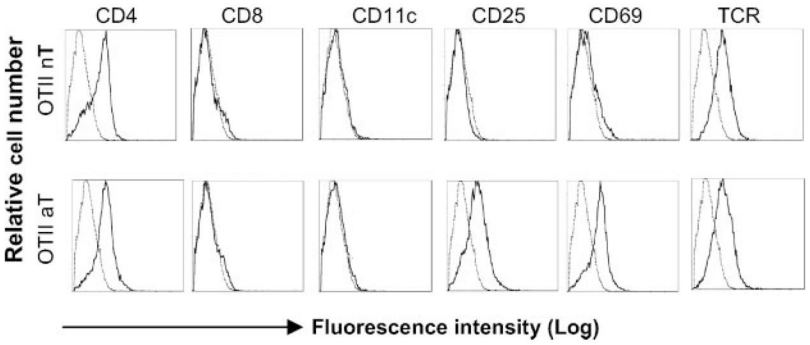

FIGURE 1.

Phenotypic analysis of $CD4^+$ T cells by flow cytometry. Flow cytometric analysis of OT II $CD4^+$ T cells. The nT OT II and aT OT II cells (thick solid lines) were stained with a panel of Abs and then analyzed by flow cytometry. These cells were also stained with isotype-matched irrelevant Abs, respectively, and used as control populations (thin dotted lines). One representative experiment of three is shown.

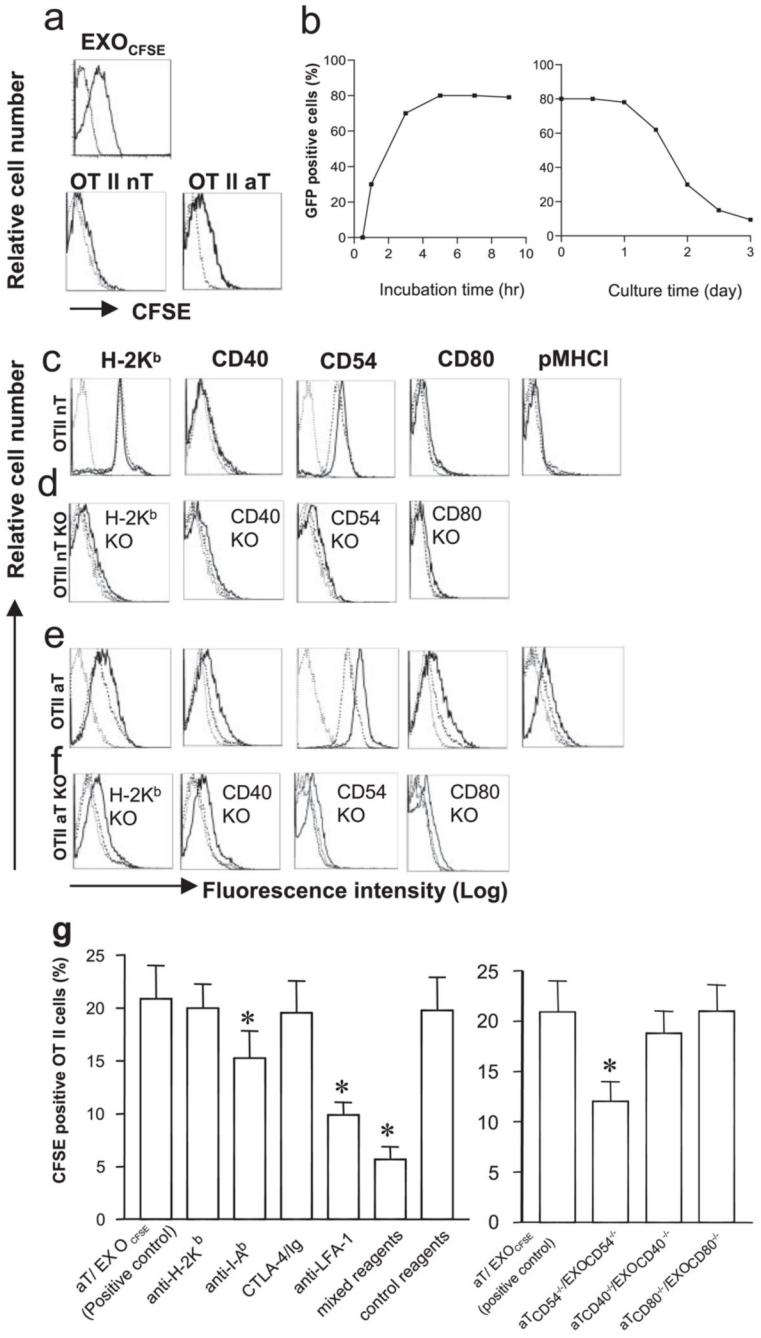

FIGURE 2.

EXO uptake by $CD4^+$ T cells. *a*, Both naive and active OT II and C57BL/6 $CD4^+$ T cells with (thick solid lines) and without (thin dotted lines) uptake of EXO_{CFSE} were analyzed for CFSE expression by flow cytometry. *b*, Kinetic study of EXO uptake by $CD4^+$ T cells. Active OT II $CD4^+$ T cells (2×10^6 cells) were incubated with EXO_{CFSE} (20 μg) in DMEM (0.2 ml) containing 10% FCS and IL-2 (10 U/ml) at 37°C for different times. CFSE-positive T cells were detected by fluorescence microscopy and the percentages of CFSE-positive T cells were calculated. In another set of experiments, active OT II $CD4^+$ T cells with incubation of EXO_{CFSE} for 5 h were cultured in DMEM containing 10% FCS and IL-2 (10 U/ml) at 37°C for different times. CFSE-positive T cells were detected by fluorescence microscopy and the

percentages of CFSE-positive T cells were calculated. *c* and *e*, Both naive and active OT II $CD4^+$ T cells with (thick solid lines) and without (thick dotted lines) uptake of EXO_{OVA} were analyzed for expression of a panel of surface molecules including $H\text{-}2K^b$, CD40, CD54, CD80, and pMHC I by flow cytometry. Irrelevant iso-type-matched Abs were used as controls (thin dotted lines). *d* and *f*, Both naive and active OT II $CD4^+$ cells from $H\text{-}2K^b$, CD40, CD54, and CD80 gene KO mice were also cocultured with (thick solid lines) and without (thick dotted lines) EXO_{OVA} and then analyzed for expression of $H\text{-}2K^b$, CD40, CD54, and CD80 by flow cytometry, respectively. Irrelevant isotype-matched Abs were used as controls (thin dotted lines). *g*, In the blocking assay, OT II $CD4^+$ aT cells were treated with anti-$H\text{-}2K^b$, anti-Ia^b, and anti-LFA-1 Abs, and CTLA-4/Ig fusion protein, a mixture of these reagents or a mixture of matched isotype Abs (as control reagents) or PBS (as positive control) on ice for 30 min, respectively, and then incubated with EXO_{CFSE}. In addition, OT II $CD4^+$ aT cells with CD54 deficiency were incubated with EXO_{CFSE} derived from CFSE-labeled ($CD54^{-/-}$) DC_{OVA}. The fractions of CFSE-positive T cells were analyzed after coculture for 5 h at 37°C. *, $p < 0.05$ vs cohorts of the positive control (aT/EXO_{CFSE}) (Student's *t* test). One representative experiment of three is displayed.

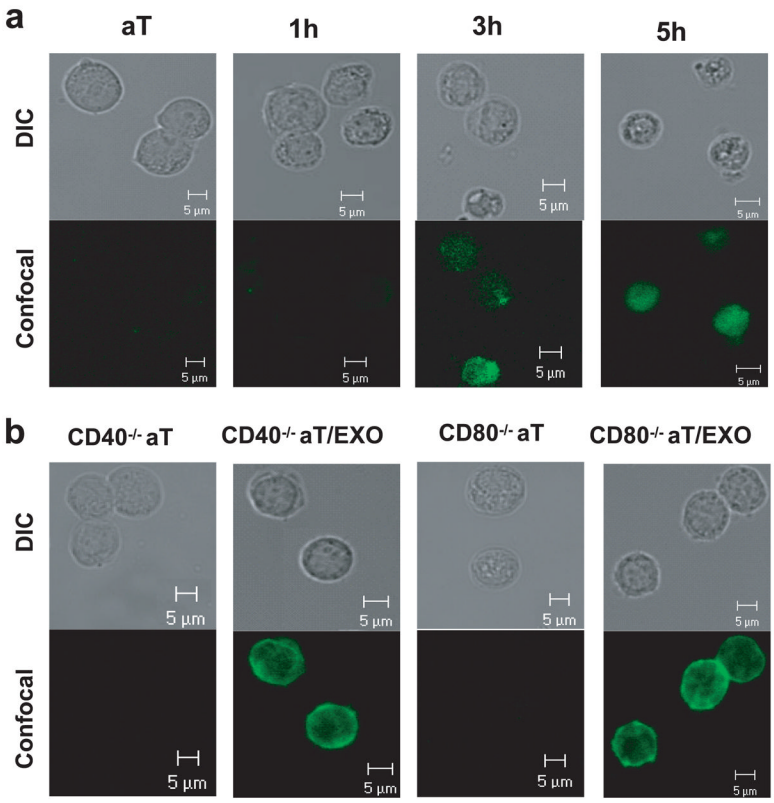

FIGURE 3.

Membrane molecule acquisition analysis by confocal fluorescence microscopy. *a*, $CD4^+$ aT cells derived from OT II mice were incubated with EXO_{CFSE} for 1, 3, and 5 h and then examined under differential interference contrast (DIC) and by confocal fluorescence microscopy. *b*, $CD4^+$ aT cells derived from OT II mice with CD40 or CD80 gene deficiency were incubated with EXO_{OVA} for 5 h, stained with FITC-conjugated anti-CD40 or anti-CD80 Ab, and then examined under DIC and by confocal fluorescence microscopy. One representative experiment of two is displayed.

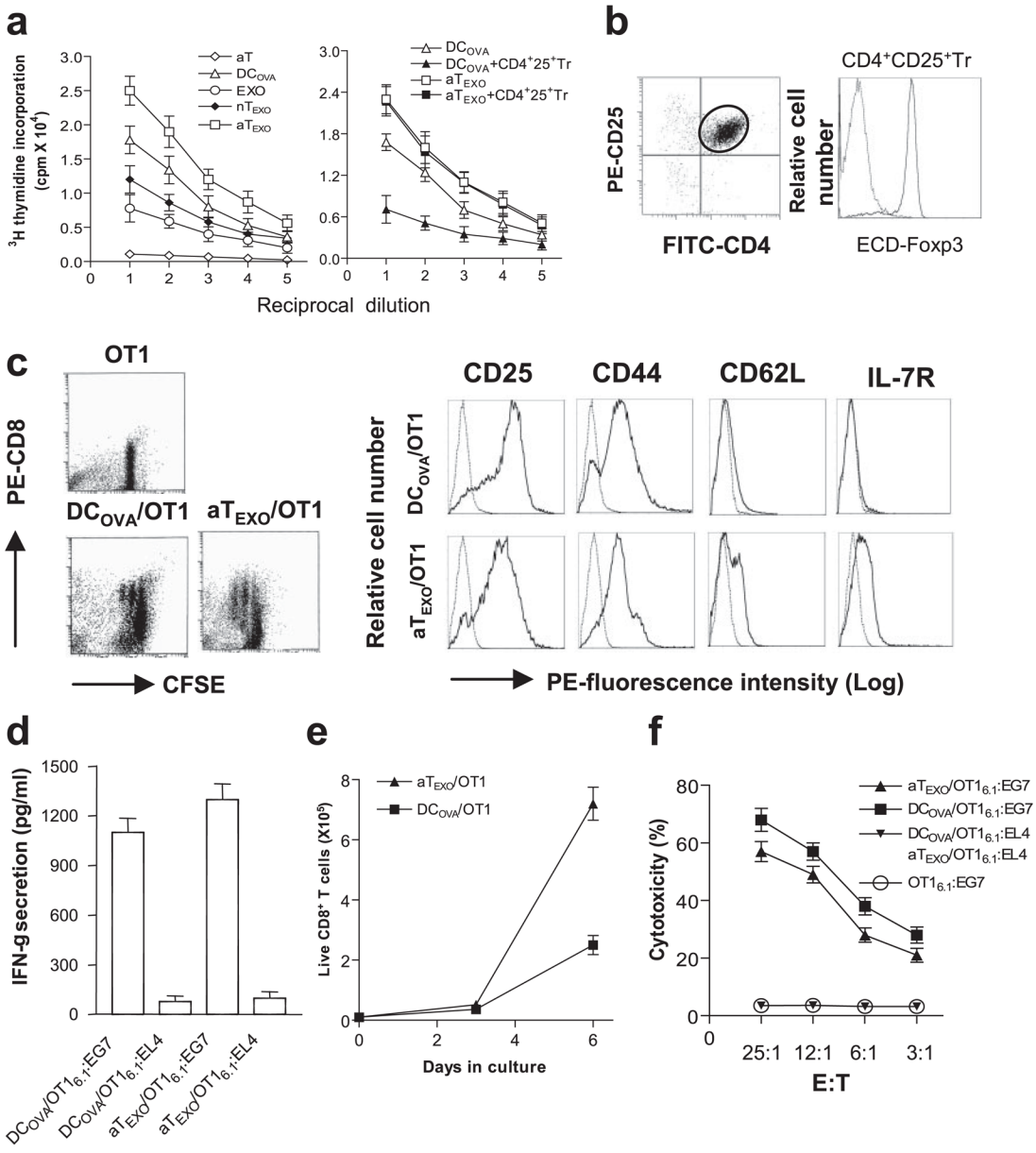

FIGURE 4.

Stimulation of CD8$^+$ memory T cell responses in vitro. *a*, In vitro CD8$^+$ cell proliferation assay. EXO$_{OVA}$ (10 μg/ml), DC$_{OVA}$, nT$_{EXO}$, aT$_{EXO}$, and Con A-activated OTII T (aT) cells and their 2-fold dilutions were cocultured with a constant number of OT I CD8$^+$T cells in presence or absence of CD4$^+$25$^+$ Tr cells. After 3 days, the proliferation response of CD8$^+$ T cells was determined by [^{3}H]thymidine uptake assay. *b*, Phenotypic analysis of CD4$^+$25$^+$ Tr cells. The CD4$^+$25$^+$ Tr cells were purified from C57BL/6 mouse splenocytes using CD25 microbeads, stained with PE-CD25, FITC-CD4, and ECD-Foxp3 Abs, and then analyzed by flow cytometry. The FITC-CD4- and PE-CD25-positive T cells were grouped for analysis of ECD-Foxp3 expression (solid line). Irrelevant isotype-matched Ab was used as a control (dotted line). *c*, Phenotypic analysis of in vitro aT$_{EXO}$-primed CD8$^+$ T cells. CFSE-labeled naive T cells derived from OT I mice were primed with irradiated DC$_{OVA}$ and aT$_{EXO}$ for 2 days in vitro and stained for CD8, CD25, CD44, CD62L, and IL-7R, respectively. Dot plots of CFSE-

positive $CD8^+$ T cells stained with PE-anti-CD8 Ab are shown, indicating that the CFSE-labeled $CD8^+$ T cells underwent some cycles of cell division, and were sorted by flow cytometry for assessment of CD25, CD44, CD62L, and IL-7R expression using PE-labeled Abs (solid lines) or PE-isotype-matched irrelevant Abs (dotted lines) by flow cytometry. *d*, The in vitro DC_{OVA}- and aT_{EXO}-activated OT I $CD8^+CD45.1^+$ T cells were purified using biotin anti-CD45.1 Ab and anti-biotin microbeads (Miltenyi Biotec) and are referred to as DC_{OVA}/OT $I_{6.1}$ and aT_{EXO}/OT $I_{6.1}$, respectively. They were then incubated with irradiated (4,000 rad) EG7 and EL4 for 24 h. The supernatants in wells containing DC_{OVA}/OT $I_{6.1}$ plus EG7 or EL4 cells (DC_{OVA}/OT $I_{6.1}$:EG7 or DC_{OVA}/OT $I_{6.1}$:EL4) and aT_{EXO}/OT $I_{6.1}$ plus EG7 or EL4 cells (aT_{EXO}/OT $I_{6.1}$:EG7 or aT_{EXO}/OT $I_{6.1}$:EL4) were examined for IFN-γ expression by ELISA. *e*, T cell proliferation assay. In vitro DC_{OVA}- and aT_{EXO}-activated $CD8^+CD45.1^+$ T cells (0.4×10^5 cells/well) derived from OT I/B6.1 mouse OTI $CD8^+$ T cells, primed on day 0 with irradiated DC_{OVA} (■) or aT_{EXO} (▲), were maintained in cultures for 1 wk with the indicated cytokines (IL-2 (50 U/ml) and IL-7 (10 ng/ml)) added on days 3 and 5. Live $CD8^+$ T cells with trypan blue exclusion for each culture done in triplicate were counted at the indicated time points. *f*, In vitro cytotoxicity assay. The above DC_{OVA}/OT $I_{6.1}$ (■) and aT_{EXO}/OT $I_{6.1}$ (▲) cells were used as effector cells, whereas ^{51}Cr-labeled EG7 or EL4 cells were used as target cells in a chromium release assay. One representative experiment of three is displayed.

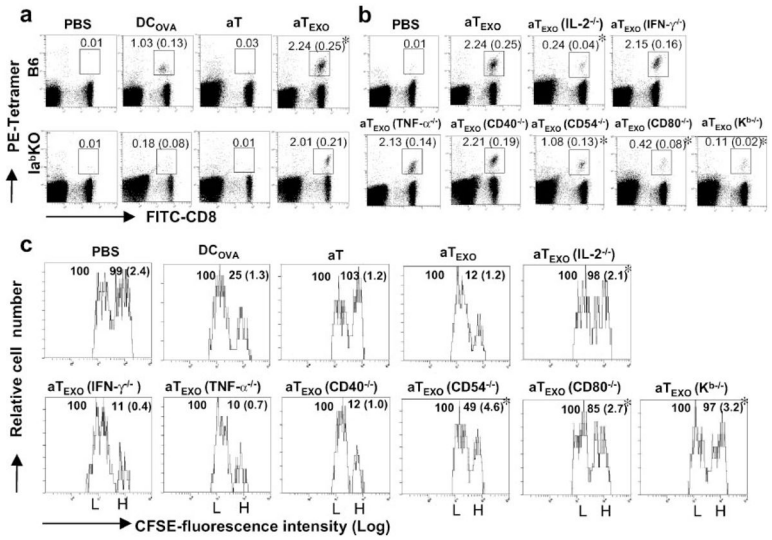

FIGURE 5.

Stimulation of $CD8^+$ T cell proliferation and differentiation into CTL in vivo. Wild-type C57BL/6 or $Ia^{b-/-}$ gene KO mice were i.v. immunized with irradiated (*a*) DC_{OVA}, aT and aT_{EXO}, and (*b*) aT_{EXO} with various gene KO, respectively. Six days after immunization, the tail blood samples of immunized mice were incubated with PE-H-$2K^b$/OVAI tetramer and FITC-anti-CD8 Ab (Beckman Coulter) according to the company's protocol, then analyzed by flow cytometry. The value in each panel represents the percentage of tetramer-positive $CD8^+$ T cells vs the total $CD8^+$ T cell population. The value in parentheses represent the SD. *, $p < 0.05$ vs cohorts of the positive control ($aT/_{EXO}$) (Student's *t* test). *c*, In an in vivo cytotoxicity assay, the above immunized mice were i.v. coinjected at a 1:1 ratio of splenocytes labeled with high (3.0 μM, $CFSE^{high}$) and low (0.6 μM, $CFSE^{low}$) concentrations of CFSE and pulsed with OVAI and Mut 1 peptide, respectively, 6 days after immunization with aT, aT_{EXO}, and aT_{EXO} with various gene KO, respectively. Sixteen hours after target cell delivery, the residual $CFSE^{high}$ and $CFSE^{low}$ target cells remaining in the recipients' spleens were sorted and analyzed by flow cytometry. The value in each panel represents the percentage of $CFSE^{high}$ cells vs $CFSE^{low}$ cells remaining in the spleens. *, $p < 0.05$ vs cohorts of the positive control (aT/EXO_{CFSE}) (Student's *t* test). One representative experiment of three in the above different experiments is shown.

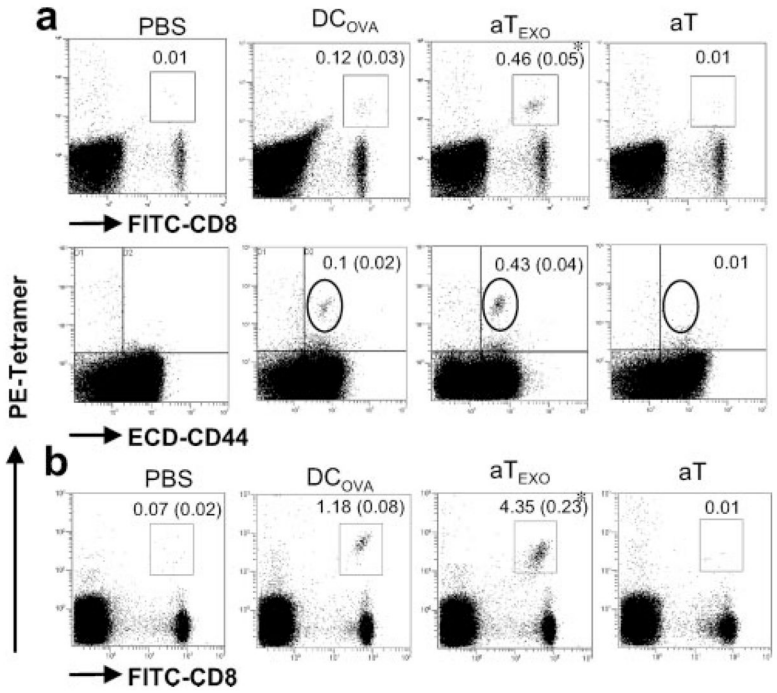

FIGURE 6.

Development of Ag-specific $CD8^+$ memory T cells. *a*, C57BL/6 mice were immunized with irradiated DC_{OVA} and aT_{EXO}, respectively. Three months later, the tail blood was taken from these immunized mice and stained with PE-H-$2K^b$/OVA tetramer, FITC-anti-CD8 and ECD-anti-CD44 Abs, and analyzed by flow cytometry. The value in each panel represents the percentage of tetramer-positive $CD8^+$ T cells vs the total $CD8^+$ T cell population. The value in parentheses represents the SD. The PE-tetramer- and FITC-CD8-positive cells in the squares were sorted and analyzed, showing they were also PE-tetramer- and ECD-CD44-positive cells in the circles. *, $p < 0.05$ vs cohorts of the positive control (DC_{OVA}) (Student's *t* test). *b*, The above immunized mice were boosted with DC_{OVA}. Four days after the boost, the recall responses were examined using staining with PE-H-$2K^b$/OVA tetramer and FITC-anti-CD8 Ab and analyzed by flow cytometry. The value in each panel represents the percentage of tetramer-positive $CD8^+$ T cells vs the total $CD8^+$ T cell population. The value in parentheses represents the SD. The results presented are representative of five separate mice per group. One representative experiment of three is shown.

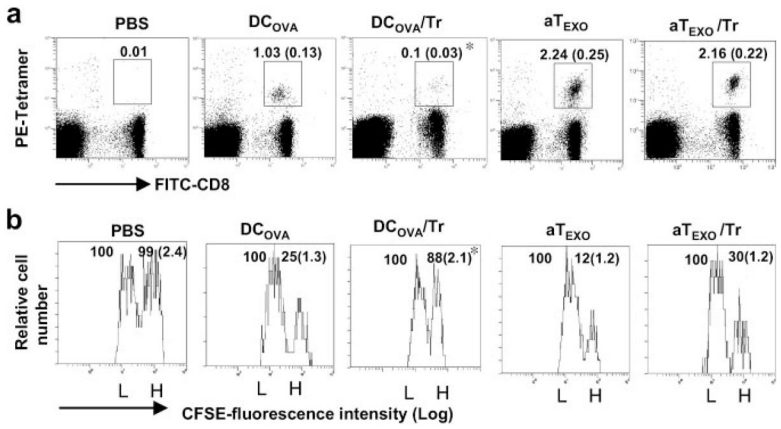

FIGURE 7.

$CD4^+25^+$ Tr-mediated suppression of $CD8^+$ T cell proliferation and differentiation in vivo. Wild-type C57BL/6 mice were i.v. immunized with irradiated (*a*) DC_{OVA}, aT and aT_{EXO}, alone or with $CD4^+25^+$ Tr cells, respectively. Six days after immunization, the tail blood samples of immunized mice were incubated with PE-H-$2K^b$/OVAI tetramer and FITC-anti-CD8 Ab according to the company's protocol, then analyzed by flow cytometry. The value in each panel represents the percentage of tetramer-positive $CD8^+$ T cells vs the total $CD8^+$ T cell population. The value in parentheses represents the SD. *, $p < 0.05$ vs cohorts of the positive control (aT_{EXO} in absence of Tr cells) (Student's *t* test). *b*, In an in vivo cytotoxicity assay, the above immunized mice were i.v. coinjected at a 1:1 ratio of splenocytes labeled with high (3.0 μM, $CFSE^{high}$) and low (0.6 μM, $CFSE^{low}$) concentrations of CFSE and pulsed with OVAI and Mut 1 peptide, respectively, 6 days after immunization. Sixteen hours after target cell delivery, the residual $CFSE^{high}$ and $CFSE^{low}$ target cells remaining in the recipients' spleens were sorted and analyzed by flow cytometry. The value in each panel represents the percentage of $CFSE^{high}$ cells vs $CFSE^{low}$ cells remaining in the spleens. *, $p < 0.05$ vs cohorts of the positive control (aT_{EXO} in absence of Tr cells) (Student's *t* test). One representative experiment of three in the above different experiments is shown.

Table I

EXO-targeted $CD4^+$ T cell vaccine protects against lung tumor metastases

Vaccines[a]	Tumor Growth Incidence (%)	Median Number of Lung Tumor Colonies
Expt. 1		
DC_{OVA}	2/8 (25)	17 ± 6
aT_{EXO}	0/8 (0)	0
aT	8/8 (100)	>100
PBS	8/8 (100)	>100
Expt. 2		
aT_{EXO}(IL-$2^{-/-}$)	7/8 (88)	78 ± 20
aT_{EXO}(IFN-$\gamma^{-/-}$)	0/8 (0)	0
aT_{EXO} (TNF-$\alpha^{-/-}$)	0/8 (0)	0
aT_{EXO} (CD$40^{-/-}$)	0/8 (0)	0
aT_{EXO} (CD$54^{-/-}$)	3/8 (38)	26 ± 8
aT_{EXO} (CD$80^{-/-}$)	5/8 (63)	47 ± 23
aT_{EXO} ($K_b^{-/-}$)	7/8 (88)	84 ± 17
PBS	8/8 (100)	>100
Expt. 3		
DC_{OVA}	4/8 (50)	14 ± 9
aT_{EXO}	0/8 (0)	0
PBS	8/8 (100)	>100
Expt. 4		
DC_{OVA}	2/8 (25)	17 ± 6
DC_{OVA} plus Tr cells	8/8 (100)	>100
aT_{EXO}	0/8 (0)	0
aT_{EXO} plus Tr cells	0/8 (0)	0
PBS	8/8 (100)	>100

[a] In experiment 1, the wild-type C57BL/6 (B6) mice ($n = 8$) were i.v. immunized with DC_{OVA}, aT and aT_{EXO} cells, or PBS. In experiment 2, the wild-type C57BL/6 mice ($n = 8$) were i.v. immunized with either aT_{EXO} cells or aT_{EXO} cells with various gene KO. Six days after the immunization, each mouse was challenged i.v. with OVA-expressing ($BL6–10_{OVA}$) tumor cells (0.5×10^6 cells/mouse). In experiment 3, the wild-type C57BL/6 mice ($n = 8$) were i.v. immunized with DC_{OVA}, aT_{EXO}, or PBS. Three months after the immunization, each mouse was challenged i.v. with $BL6–10_{OVA}$ tumor cells (2×10^6 cells/mouse). In experiment 4, the wild-type C57BL/6 mice ($n = 8$) were i.v. immunized with DC_{OVA}, aT_{EXO} cells alone or together with $CD4^+25^+$ Tr cells. Six days after the immunization, each mouse was challenged i.v. with OVA-expressing ($BL6–10_{OVA}$) tumor cells (0.5×10^6 cells/ mouse). All the mice were sacrificed 4 wk after tumor cell challenge and the numbers of lung metastatic tumor colonies were counted. One representative experiment of three is shown.